Inhibition of the ATG4-LC3 pathway suppressed osteoclast maturation

日浦, 史隆

Biochemical and Biophysical Research Communications 632 (2022) 40–47

Contents lists available at ScienceDirect

Biochemical and Biophysical Research Communications

journal homepage: www.elsevier.com/locate/ybbrc

Inhibition of the ATG4-LC3 pathway suppressed osteoclast maturation

Fumitaka Hiura [a], Yuko Kawabata [b], Tsukasa Aoki [a], Akiko Mizokami [c], Eijiro Jimi [a, c, *]

[a] Laboratory of Molecular and Cellular Biochemistry, Division of Oral Biological Sciences, Faculty of Dental Science, Kyushu University, 3-1-1 Maidashi, Higashi-ku, Fukuoka, 812-8582, Japan
[b] Department of Cell Biology, Aging Science, and Pharmacology, Division of Oral Biological Sciences, Faculty of Dental Science, Kyushu University, 3-1-1 Maidashi, Higashi-ku, Fukuoka, 812-8582, Japan
[c] Oral Health/Brain Health/Total Health Research Center, Faculty of Dental Science, Kyushu University, 3-1-1 Maidashi, Higashi-ku, Fukuoka, 812-8582, Japan

ARTICLE INFO

Article history:
Received 9 September 2022
Received in revised form
12 September 2022
Accepted 15 September 2022
Available online 20 September 2022

Keywords:
Osteoclasts
ATG4B
LC3
Autophagy

ABSTRACT

Autophagy is a non-selective action in which cells degrade parts of themselves, reusing degraded cellular components. Among autophagy-related gene (ATG) family members, ATG4 proteins play crucial roles in the microtubule-associated protein 1 light chain 3 (LC3) phosphatidylethanolamine (PE) system which is essential for autophagosome maturation. Although autophagy has been shown to be involved in osteoclastic bone resorption, the role of ATG4/LC3 in bone resorption remains unclear. When mouse bone marrow cells were treated with various concentrations of NSC185058 (NSC), a specific inhibitor of ATG4B, 1 h prior to treatment with receptor activator of NF-κB ligand (RANKL) in the presence of macrophage colony stimulating factor (M-CSF), NSC inhibited osteoclastogenesis in a dose-dependent manner. Addition of NSC in the late stages of osteoclast differentiation suppressed multinucleation and reduced the expression of markers for mature osteoclasts such as *Dc-stamp*, *Mmp9*, and *Ctsk*. NSC also suppressed actin ring formation and pit formation in mature osteoclasts. When a periodontitis model involving eight-week-old male mice in which the right maxillary second molar had been ligated with silk thread was injected with or without NSC, alveolar bone resorption was suppressed by a decrease in the number of osteoclasts in the NSC-treated group. These results suggest that LC3 is important for the maturation of osteoclasts and that LC3 inhibition is a new therapeutic strategy for periodontal disease.

1. Introduction

Osteoclasts are differentiated from hematopoietic stem cells and resorb bone [1,2]. Osteoclastic bone resorption consists of two steps, osteoclast differentiation and osteoclastic bone resorption. Osteoclast differentiation is induced by receptor activator of NF-κB ligand (RANKL) produced by osteoblasts and osteocytes. Once RANKL binds RANK, a receptor of RANKL expressed on the cell surface of osteoclast precursors, NF-κB or mitogen-activated protein kinase (MAPK) is activated and finally induces nuclear factor of activated T cell 1 (NFATc1) expression, which is a master regulator of osteoclastogenesis. NFATc1 induces the expression of osteoclast differentiation markers. Mono- or bi-nuclear osteoclasts fuse with each other and then become multinucleated osteoclasts via *Dcstamp* expression. Those multinucleated osteoclasts then recognize bone surface and polarize via Src activation and secrete proton and proteinases, such as cathepsin K (CathK) or matrix metalloproteinase (MMP9), underneath ruffled border to resorb bone matrix. Activated osteoclasts form an actin ring structure correlated with the sealing zone, and its formation reflects bone resorption activity [1,2].

Autophagy is the basic intracellular degradation system that is universally conserved in eukaryotes [3,4]. In autophagy, various cellular components are sequestered in double-membrane vesicles (vesicles separated by two lipid bilayers) called “autophagosomes”, transported to lysosomes or vacuoles, and degraded. Autophagy has two characteristics—a diversity of degradation targets and a

Abbreviations: RANKL, receptor activator of NF-κB ligand; M-CSF, macrophage colony stimulating factor; TRAP, tartrate-resistant acid phosphatase; ATG, autophagy-related gene; LC3, microtubule-associated protein 1 light chain 3; PE, phosphatidylethanolamine.

* Corresponding author. Oral Health/Brain Health/Total Health Research Center, Faculty of Dental Science, Kyushu University, 3-1-1 Maidashi, Higashi-ku, Fukuoka, 812-8582, Japan.
E-mail address: ejimi@dent.kyushu-u.ac.jp (E. Jimi).

https://doi.org/10.1016/j.bbrc.2022.09.065
0006-291X/

certain degree of selectivity—and is responsible for maintaining intracellular homeostasis and various physiological functions, such as intracellular immunity, development, and differentiation [3,4]. The formation of autophagosomes is carried out by 18 major autophagy-related gene (ATG) proteins [3,4]. ATG4 proteins are cysteine proteases that regulate the microtubule-associated protein 1 light chain 3 (LC3) phosphatidylethanolamine (PE) system, which is essential for autophagosome maturation [5]. In humans, there are four ATG4 homologs: ATG4A, ATG4B, ATG4C, and ATG4D; of these four homologs, ATG4B shows the most effective cleavage for LC3 [6]. ATG4B not only cleaves the initiate produced LC3 into form-I (LC3-I) and prepares it for conjugating to PE, which is essential for elongation of the isolation membrane, but also contributes to the deconjugation of LC3-PE, releasing LC3 for recycling during autophagosome development [7,8]. Both upregulation and down-regulation of ATG4B result in abnormal autophagy progression, and the loss-of-function of ATG4B is involved in the development of many human diseases [4,9–11].

Several lines of evidence have shown the importance of autophagy in the osteoclast differentiation and function [12,13]. Expression of autophagy proteins has been shown to be increased during osteoclast differentiation. For example, the expression of ATG 5/7/12 and the LC3-II/LC3-I ratio increased with degradation of p62 (SQSTM1/sequestome1) during RANKL-induced osteoclast differentiation [14]. Autophagy-associated proteins, including ATG5, ATG7, ATG4B, LC3, and Beclin-1, a mammalian homolog of yeast ATG6, were found to be important for osteoclast activity, as they regulate ruffled border formation, lysosomal trafficking, and secretion of lysosomal enzymes, both *in vitro* and *in vivo* [15]. Autophagy inhibitors and knockdown of autophagy-related proteins have been reported to suppress osteoclast differentiation and osteoclast activation [12,13,16]. Furthermore, autophagy-associated protein gene-deficient mice showed an increase in trabecular bone mass under the inhibition of bone resorption, suggesting that inhibiting the function of autophagy-associated proteins is a good therapeutic target for bone destruction-associated diseases, such as osteoporosis, rheumatoid arthritis and periodontitis [12,13].

Periodontal disease is a chronic inflammatory disease characterized by destruction of periodontal tissue initiated by pathogenic bacterial infections and interacting with host immune defenses to cause inflammation and alveolar bone resorption [2,17]. In previous studies, the autophagy level of periodontal ligaments was increased in patients with periodontitis compared with healthy controls [18]. Autophagy plays an important role in regulating osteoclast differentiation and its function in alveolar bone resorption, as well as in regulating host inflammatory and immune responses to periodontal pathogenic bacterial stimulation [19]. Maintaining autophagic homeostasis may be an effective therapeutic approach to control the host response and alveolar bone resorption in periodontal disease.

In this study, we investigated the effect of a selective inhibitor of ATG4B among the ATG proteins that regulate autophagy, on osteoclastic bone resorption and its potential utility as a therapeutic agent for bone loss of periodontal disease.

2. Materials and methods

2.1. Reagents

Glutathione S-transferase (GST)-RANKL and NSC185058 were purchased from Oriental Yeast Company, Ltd. (Shiga, Japan) and Selleck Chemicals (Houston, TX, USA), respectively. Recombinant human macrophage-stimulating factor (M-CSF) was purchased from FUJIFILM Wako Pure Chemical Corporation (Osaka, Japan). Anti-LC3A/B (4108s) and anti-β-actin (AC-15) antibodies were obtained from Cell Signaling Technology (Beverly, MA, USA) and Sigma-Aldrich (St. Louis, MO, USA), respectively.

2.2. Mice

The handling of the mice and all procedures were approved by the Animal Care Committee of Kyushu University, according to the guidelines of the National Research Council's Guide for the Care and Use of Laboratory Animals, and the Japanese Council on Animal Care (Approval Number: A30-209-0, A22-203-0).

2.3. Osteoclastogenesis

Bone marrow cells from femurs and tibiae of 8-week-old male C57BL6/J mice were prepared and cultured for 6 days in the presence of various concentrations of NSC185058 together with M-CSF (50 ng/ml) and RANKL (50 ng/ml) in α-minimal essential medium (α-MEM) containing 10% fetal bovine serum (FBS) and antibiotics (100 units/ml penicillin, and 100 μg/ml streptomycin) in 48-well plates. The medium was changed every 2 days and NSC185058 was added 1h before RANKL stimulation. On day 6 of culture, cells were fixed with 3.7% formaldehyde in phosphate-buffered saline (PBS) for 10 min. After permeabilization with 0.1% Triton X-100, cells were stained with tartrate-resistant acid phosphatase (TRAP) and 0.3 mM Alexa488-labeled phalloidin. Cells were observed under a microscope and TRAP-positive multinucleated cells (MNC) were counted as osteoclasts. The distribution of F-actin was detected by fluorescence microscopy using BIOREVO BZ-9000 microscope (Keyence, Keyence, Osaka, Japan).

2.4. The cell viability assay

To examine the effects of NSC185058 on cell viability, bone marrow cells were cultured for the indicated period in the presence of various concentrations of NSC185058 and 10 μl of CCK-8 solution was added to each well on day 2, 4, 6 of culture, using the CCK-8 kit (Dojindo Molecular Technologies, Inc., Shiga, Japan), according to the manufacturer's protocol. The plates were incubated at 37 °C for 4 h, and then, the absorbance was then measured at a wavelength of 450 nm.

2.5. Quantitative real-time polymerase chain reaction (PCR)

Total RNA prepared using the Relia Prep™ RNA Cell Miniprep system (Promega, Madison, WI, USA) was transcribed to cDNA using the High Capacity cDNA Reverse Transcription Kit (Applied Biosystems, Foster City, CA, USA). The cDNA was further subjected to real-time PCR using KOD SYBR qPCR Mix (Toyobo, Osaka, Japan) and Thermal Cycler Dice Real Time System II (TaKaRa, Shiga, Japan). The GAPDH expression served as an internal control.

Primer sequences were as follows: *Nfatc1*, 5′-GTTGGTATTAAAATTCTGAAACC-3′ (forward) and 5′-TTGCTGCCCTTTCACTGATG-3′ (reverse); *c-Src*, 5′- GTTGCTTCGGAGAGGTGTGGAT-3′ (forward) and 5′- CACCAGTTTCTCTCGTGCCTCAGT-3′ (reverse); *Dcstamp*, 5′-CCGTGGGCCAGAAGTTGC-3′ (forward) and 5′-GCCAGTGCTGACTAGGATG-3′ (reverse); *Mmp9*, 5′-GGACCCGAAGCGGACATTG-3′ (forward) and 5′- CGTCGTCGAAATGGGGCATC-3′ (reverse); *Ctsk*, 5′-GAAGAAGACTCACCAGAAGC-3′ (forward) and 5′-GGTTATGGGCAGAGATTTGC-3′ (reverse); *Gapdh*, 5′-AACTTTGGCATTGTGGAAGG-3′ (forward) and 5′-ACACATTGGGGGTAGGAACA-3′ (reverse).

2.6. Western blot analyses

Total cell lysates were prepared using TNE lysis buffer (10 mM Tris, pH 7.8, 150 mM NaCl, 1 mM EDTA, 1% Nonidet P-40, and 1 mM

dithiothreitol) containing proteinase inhibitor cocktail (Promega, Madison, WI, USA). Each lysate was resolved on 10% sodium dodecyl sulfate polyacrylamide gel electrophoresis (SDS-PAGE) gels, and transferred to Immobilon-P membranes (Merck Millipore, Darmstadt, Germany). After blocking with TBS-T solution containing 5% skimmed milk, the membrane was immunoblotted with individual primary antibodies overnight at 4 °C, followed by incubation with horseradish peroxidase-conjugated secondary antibodies (Cell Signaling Technology). The immunoreactive proteins were visualized using an ImmunoStarLD (FUJIFILM Wako Pure Chemical), and analyzed with an ImageQuant LAS 4000 mini (GE Healthcare, Chicago, IL, USA).

2.7. Coculture and pit formation

Primary osteoblasts (POBs) were obtained from the calvariae of newborn C67BL6/J mice by digestion with 0.1% collagenase (FUJIFILM Wako Pure Chemical) and 0.2% dispase (Godo Shusei, Tokyo, Japan). Bone marrow cells obtained from 8-week-old male C67BL6/J male mice were cocultured with POBs in α-MEM containing 10% FBS, 1α,25-dihydroxyvitamin D_3 [1α,25$(OH)_2D_3$] (10^{-8} M) (FUJIFILM Wako Pure Chemical) and prostaglandin E_2 (10^{-7} M) (Sigma) in culture dishes (Φ100 mm) coated with collagen gel (Nitta Gelatin, Osaka, Japan). Osteoclasts were removed from the dishes by treating them with 0.2% collagenase (FUJIFILM Wako Pure Chemical). Mature osteoclasts were seeded onto dentin slices (Φ6 mm; MS Labo System, Kanagawa, Japan) and further cultured for 48 h in α-MEM containing 10% FBS with or without various concentrations of NSC185058 in 48-well plates. After cells were removed from the dentine slices, and the slices were stained with Mayer's hematoxylin. The area of each pit was acquired using BIOREVO BZ-9000 microscope (Keyence, Keyence, Osaka, Japan) and measured with the image analysis software program (BZ-X800 Analyzer; Keyence). To examine the actin ring formation, formed osteoclasts were seeded onto dentin slices for 24 h and then stained for TRAP and 0.3 mM Alexa488-labeled phalloidin.

2.8. Ligature-induced periodontitis model

Eight-week-old male C57BL6/J mice were randomly divided into 3 groups to receive the following treatments: (1) control group (unligated + PBS, n = 10), (2) ligated group (ligated + DMSO, n = 9), and (3) NSC185058 group (ligated + NSC185058, 1.451 μg/kg, n = 10). A mouse periodontitis model was performed by tying a 6-0 silk ligature (Akiyama Medical Mfg. Co., Ltd., Tokyo, Japan) around the left maxillary second molar according to Abe et al. [20]. After ligation, either DMSO or NSC185058 dissolved in DMSO (20 μl) was injected in two places of the palatal gingiva of the ligated second maxillary molar using a Hamilton syringe with a 33-gauge needle (Hamilton Company, Reno, NV, USA). After 7 days, the mice were euthanized and the maxillae were removed for following experiments.

2.9. Radiological assessments

All dissected maxillary bones were fixed with 4% paraformaldehyde in a PBS (pH 7.4) for 24 h, at 4 °C and washed with PBS several times. The bone mineral densities (BMDs) and three-dimensional (3D) reconstructed images of the maxillary bone were acquired using micro-focal computed tomography (μCT; ScanXmate-L090T, Comscan Co, Kanagawa, Japan).

2.10. Histological preparation and bone histomorphometry

Maxilla were fixed with 4% paraformaldehyde and decalcified with Osteosoft (Merck, Darmstadt, Germany). Sagittal paraffin sections (5 μm thick) were cut. Sections were analyzed with TRAP staining. Sections were analyzed using a BZ-9000 (Keyence). Osteoclasts were recognized as $TRAP^+$ MNCs that contained three or more nuclei on the bone surface. The resorbed area was measured using an image analysis software program (BZ-X800 Analyzer; Keyence).

2.11. Statistical analyses

Data are shown as the mean ± standard deviation (SD). Comparisons of the means between two groups were carried out using a *t*-test (vs. control; *P < 0.05, **P < 0.01). When evaluating more than two groups, statistical comparisons were performed by an analysis of variance (ANOVA) with Tukey's test for multiple comparisons. *P < 0.05, **P < 0.01. Statistical analyses were performed with the SPSS software package version 27.0 (IBM, Armonk, NY, USA).

3. Results

3.1. NSC185058, a selective inhibitor of ATG4B suppresses RANKL-induced osteoclastogenesis

To investigate the physical role of AGT4B in RANKL-induced osteoclastogensis, we pretreated bone marrow macrophages (BMMs) with various concentrations of NSC185058, a specific inhibitor of AGT4B, and then treated them with RANKL for six days. NSC185058 inhibited RANKL-induced osteoclastogenesis in a dose-dependent manner (Fig. 1A and B). ATG4 is involved in the cleavage of pro-LC3 and the degreasing of LC3-PE [7,8]. Thus, inhibition of ATG4B leads to the accumulation of lipidated LC3 (LC3-II). RANKL induced LC3-II expression, and pretreatment with NSC185058 further induced LC3-II accumulation in a dose dependent manner (Fig. 1C). NSC185058 at 10 μM completely inhibited RANKL-induced osteoclastogenesis. Although the number of living cells was not affected in the presence of up to 5.0 μM of NSC185058, NSC185058 at 10 μM induced cell death (Fig. 1D). Thus, we used NSC185058 at 5 μM to examine the expression of osteoclast differentiation markers, including *Nfatc1, Dcstamp, c-Src, Ctsk,* and *Mmp9*. NSC185058 hardly suppressed the expression of *Nfatc1*, which is an early differentiation marker of osteoclasts, but suppressed the expression of *Dcstamp, c-Src, Ctsk,* and *Mmp9*, which are late differentiation markers (Fig. 1E). These results are consistent with the induction of small osteoclasts without actin rings by pretreatment with NSC185058 (Fig. 1A).

3.2. NSC185058 suppresses maturation of osteoclasts

The findings concerning the expression of osteoclast differentiation markers suggest that NSC185058 suppresses the late differentiation of osteoclastogenesis. Therefore, the osteoclast differentiation induction period of 6 days was divided into an early stage, middle stage, and late stage, and NSC185058 was added as shown in Fig. 2A. Osteoclast differentiation was suppressed by adding NSC185058 from the middle stage to the late stage as shown in Fig. 2B and C, suggesting that NSC185058 suppressed the late differentiation stage of osteoclasts.

3.3. NSC185058 suppresses the bone resorption by mature osteoclasts

Since NSC185058 suppressed the late differentiation of osteoclasts, we investigated the possibility of suppressing the bone resorption function by mature osteoclasts. Coculture of mouse bone

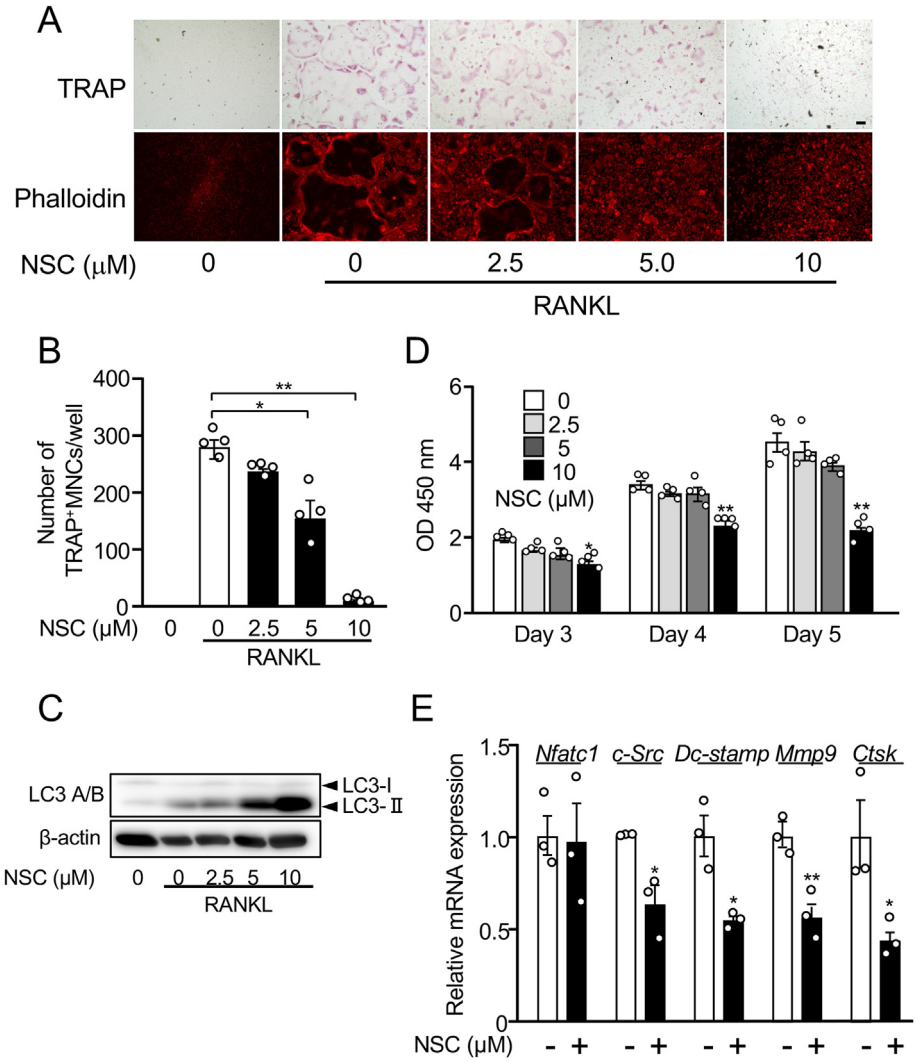

Fig. 1. NSC185058 suppresses RANKL-induced osteoclastogenesis. Mouse bone marrow cells were cultured with M-CSF (100 ng/ml) and RANKL (100 ng/ml) for 6 days. Various concentrations of NSC185058 were added 1h before RANKL stimulation. (A) Cells were stained by TRAP and Alexa488-labeled phalloidin. Scale bar = 100 μm. (B) The number of $TRAP^+$MNCs was counted. Data are expressed as the mean ± SD (n = 4). (C) A Western blot analysis was used to determine the expression of LC3A/B, with β-actin used as a loading control. (D) After 3, 4, and 5 days of culture, the cell viability was analyzed using a CCK-8 kit. Absorbance was measured at a wavelength of 450 nm. Data are expressed as the mean ± SD (n = 4). *P < 0.05, **P < 0.001. (E) The number of $TRAP^+$MNCs was counted. (E) After 6 days of osteoclast culture, total RNA was isolated. The mRNA expression of *Nfatc1*, *c-Src*, *Dcstamp*, *Mmp9*, *Ctsk*, and *Gapdh* was analyzed by real-time polymerase chain reaction. Data are expressed as the mean ± SD (n = 3). *P < 0.05, **P < 0.001. Similar results were obtained from three independent experiments.

marrow cells and osteoblasts was performed on collagen gel, and the formed mature osteoclasts were further cultured on dentin slices in the presence or absence of NSC185058 for 24 h, and measured the ratio of osteoclasts with actin rings. The resorbed area was also measured for 48 h.

NSC185058 at 5 μM showed little change in the number of osteoclasts, but the ratio of osteoclasts with actin rings was significantly reduced (Fig. 3A–C). NSC185058 at 10 μM induced a slight decrease in the number of osteoclasts and decreased the ratio of osteoclasts with an actin ring and the area resorbed by mature osteoclasts (Fig. 3). In the coculture, the effective concentration was different from Fig. 1A, may be due to the short culture period and the presence of a large number of osteoblasts compared to osteoclast formation. NSC185058 reduced the ratio of osteoclasts with an actin ring and the bone-resorbing activity by mature osteoclasts in a dose-dependent manner (Fig. 3).

3.4. NSC185058 prevents alveolar bone loss in periodontitis models

Since NSC185058 suppresses both osteoclast differentiation and the bone-resorbing activity, we next investigated whether or not it could suppress alveolar bone loss, using a periodontitis model. A periodontitis model was prepared by ligating a silk thread to the upper second molar of the maxillary bone of a mouse. After ligation, NSC185058 was locally injected via the buccal gingiva every three days. The area of resorbed bone was measured after one week. Three-dimensional μCT images showed less alveolar bone loss in the NSC185058-treated group than control group (Fig. 4A and B). The sagittal view of alveolar bone resorption showed that the destruction of alveolar bone was suppressed by treatment with NSC185058 (Fig. 4C and D). Consistent with these results, a histological analysis showed a reduced number of $TRAP^+$ osteoclasts in the alveolar bone in the NSC185058-treated group (Fig. 4E and F).

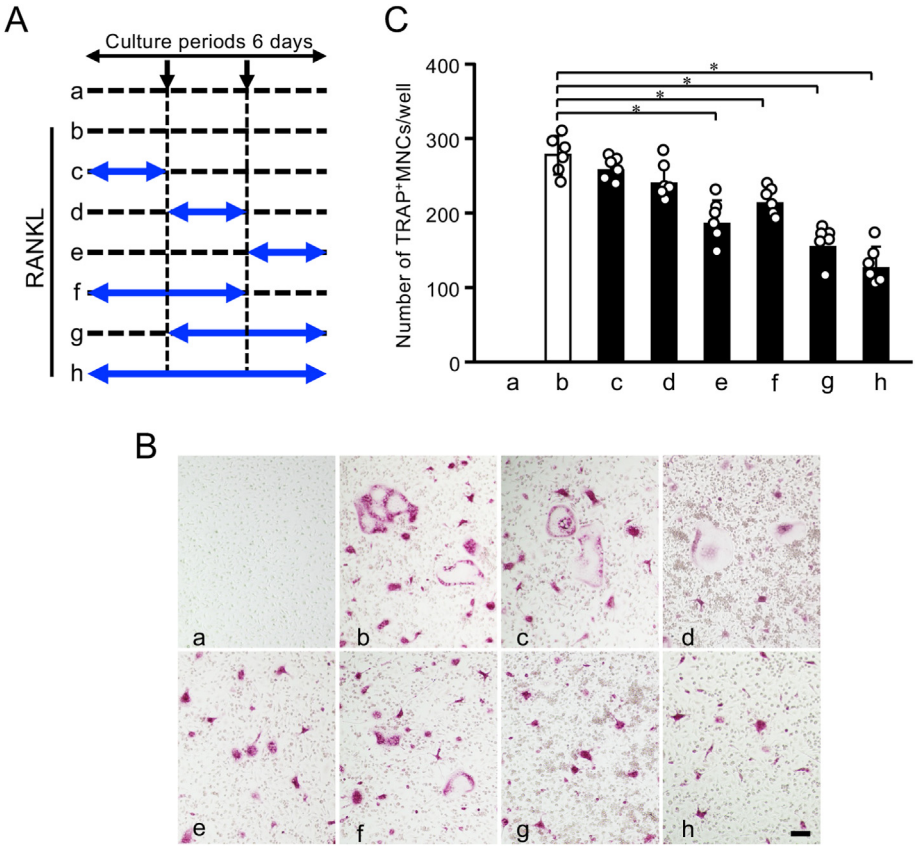

Fig. 2. Effects of temporal addition of NSC185058 on RANKL-induced osteoclastogenesis. (A) Mouse bone marrow cells were pretreated with or without various concentrations of NSC185058 for 1h and then stimulated by RANKL (100 ng/ml) for the indicated duration. (B) Cells were stained by TRAP and Alexa488-labeled phalloidin. Scale bar = 100 μm. (C) The number of TRAP⁺MNCs was counted. Data are expressed as the mean ± SD (n = 6). *P < 0.05, **P < 0.001. Similar results were obtained from three independent experiments.

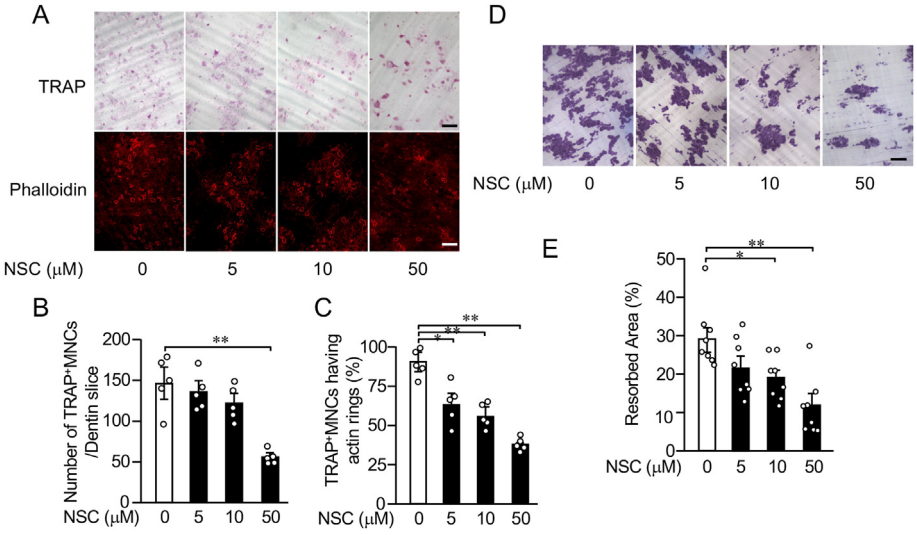

Fig. 3. NSC185058 suppresses the bone-resorbing activity of mature osteoclasts. (A) Bone marrow cells and primary osteoblasts were cocultured on a collagen gel to differentiate into osteoclasts for 7 days, and mature osteoclasts were then cultured on dentin slices with or without various concentrations of NSC185058 to evaluate the bone resorption function. Cells were stained by TRAP and Alexa488-labeled phalloidin. Scale bar = 200 μm. (B) The number of TRAP⁺MNCs (B) and TRAP⁺MNCs with actin rings (C) was counted. Data are expressed as the mean ± SD (n = 5). (D) Cells were removed from dentin slices, and the slices were stained with Mayer's hematoxylin to evaluate resorption pits. Scale bar = 200 μm. (E) The resorption pit areas were quantified using the image analysis software program. Data are expressed as the mean ± SD (n = 8). *P < 0.05, **P < 0.001. Similar results were obtained from three independent experiments.

4. Discussion

Previous studies have shown that 18 ATG proteins are involved in autophagosome formation. Among the eight types of ATG proteins, about half form two ubiquitin-like binding forms: the Atg8 binding form and the ATG12 binding form [3,4]. ATG protein is involved in bone resorption by osteoclasts according to the results of functional inhibition experiments on ATG protein [12,13]. For example, osteoclast-specific *Atg5*-deficient mice have been shown that Atg5 is important for the ruffled border formation of osteoclast without affecting osteoclast differentiation [15]. *Atg7*-deficient mice have impaired cathepsin K secretion and reduced bone resorption [21]. In contrast, Beclin-1 was shown to be upregulated during osteoclast differentiation, and Beclin-1 siRNA inhibits osteoclast differentiation by suppressing RANKL-induced activation of p38 and JNK [22]. Furthermore, the osteoclast-specific deletion of Beclin-1 increased bone mass due to decreased number of osteoclasts [23]. As described above, since each ATG protein has its own function, some ATG proteins are involved in regulation of osteoclast differentiation, and some are involved in the bone resorption function [12,13]. In the present study using NSC185058 [24], a selective inhibitor of AGT4B that plays an important role in LC3 lipidation and recycling to LC3, we demonstrated that the AGT4B/LC3 axis was important for osteoclast differentiation and bone resorption both *in vitro* and *in vivo*.

LC3 exists in two forms (cytosolic LC3-I and lipidated-LC3-II), and the presence of LC3-II indicates activation of autophagy [3,4]. Similar to previous studies, the present study also found an increase in the LC3-II type in RANKL-induced osteoclastogenesis [16]. Previous experiments with LC3 siRNA showed that knockdown of LC3 had little effect on osteoclastogenesis, suggesting that LC3 contributes to actin ring organization downstream of microtubules in a Cdc42-specific manner and is involved in bone resorption [16]. ATG4B not only plays an important role in the LC3-PE system that is essential for autophagosome maturation but also contributes to LC3-PE uncoupling and releases LC3 for recycling [7,8]. NSC185058 used in the present study induced the accumulation of lipidated-LC3 as well as other ATG4B inhibitors [25,26]. Although LC3 knockdown did not affect RNAKL-induced osteoclastogenesis [16], NSC185058 inhibited the late stage of osteoclast differentiation by accumulating lipidated-LC3. These results suggest that the balance between lipidation and recycling of LC3 may be important for osteoclast maturation.

We also examined the effect of NSC185058 on the bone resorption activity of mature osteoclasts. This experiment used coculture of osteoblasts and bone marrow cells on collagen gel to prepare mature osteoclasts as a cell suspension and seed them onto dentin slices [27]. In mature osteoclasts with osteoblasts, 5 μM of NSC185058, which suppresses osteoclast differentiation, tended to suppress actin ring formation and pit formation, but 10 μM of NSC185058 showed a significant the inhibitory effects. The difference in the concentration of NSC185058 showing an inhibitory effect between osteoclastogenesis and bone resorption by mature osteoclasts may be due to the fact that osteoblasts support the osteoclast survival [28]; alternatively, higher concentrations of NSC185058 may be required to suppress autophagosome formation in mature osteoclasts. Using the same experimental system, we previously reported that wortmannin, an inhibitor of PI3K, which is important for the conversion of LC3-1 to LC3-II [29], suppressed osteoclast actin ring formation and resorption pit formation [30,31]. These results suggest that ATG4B-induced changes in the ratio of LC3-II/LC3-1 are involved in the formation of actin rings and resorption pits in osteoclasts.

Since NSC185058 inhibits osteoclast differentiation and the bone resorption function, we investigated the possibility that

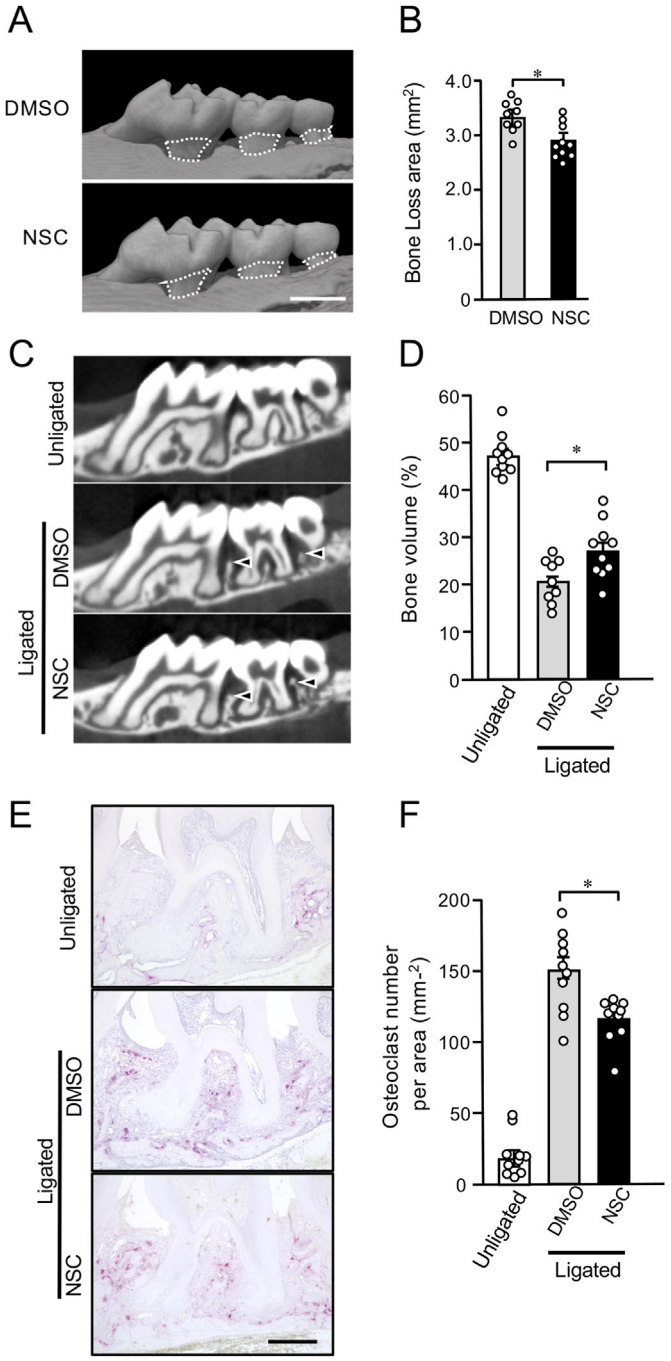

Fig. 4. NSC185058 treatment suppresses trabecular bone loss in a periodontitis model *in vivo*. A 5-0 silk ligature was ligated around the maxillary second molar of C57BL/6 mice, and from the same day, control group (DMSO) and NSC185058 were administered once every two days for 7 days. (A) Representative three-dimensional μCT images of the maxilla in each treatment group 7 days after ligature placement. Scale bar = 1 mm. (B) The area from the cement-enamel junction (CEJ) to the apex of alveolar bone (AB) on μCT images was measured using the image analysis software program. Data are expressed as the mean ± SD (n = 9–10). (C) Representative three-dimensional μCT images of the sagittal view of alveolar bone resorption. Scale bar = 1 mm. (D) The remaining the alveolar bone between the first and second molars and between the second and third molars (arrow heads) was measured using the image analysis software program. (E) TRAP staining for the presence of osteoclasts from periodontal tissue. Bone resorption was confirmed by the detection of osteoclasts. Scale bar = 300 μm. (F) The number of TRAP-positive osteoclasts per area (mm^2) was counted. TRAP-positive MNCs were counted from her two random coronal sections of ligated molars of five male mice in each group. Data are expressed as the mean ± SD (n = 10). *p < 0.05, **p < 0.01. Similar results were obtained from three independent experiments.

NSC185058 inhibits bone resorption in periodontal disease models. Autophagy plays an important role in the differentiation and function of not only osteoclasts but also other osteoblasts, osteocytes, and chondrocytes, so various side effects must be considered during systemic administrations [13]. Therefore, we selected a periodontal disease model as a bone destruction model that allows local administration, which is considered to be associated with fewer side effects than systemic administration. Autophagy in periodontal tissue is reportedly involved in the onset of periodontal disease and alveolar bone destruction [17], and indeed, conventional autophagy inhibitors chloroquine (CQ) and 3-methyladenine (3-MA) inhibited alveolar bone resorption by inhibiting osteoclastogenesis in a mouse periodontitis model [32]. The administration of NSC185058 inhibited alveolar bone resorption and significantly inhibited bone loss in the inter-root septum in a periodontitis model. A histological analysis also showed a significant reduction in osteoclast numbers. Taken together, these findings suggest that NSC185058 may become a viable option for treating periodontal disease, in addition to CQ and 3-MA.

To clarify the role of the ATG4B/LC3 axis in osteoclast differentiation and bone resorption, we further needed to investigate *Atg4b*- or *LC3*-deficient mice. Conventional *Atg4b*-deficient mice had significantly reduced autophagy activity systemically [33]. Mouse embryonic fibroblasts derived from *Atg4b*-deficient mice failed to form LC3-II and inhibited autophagosome maturation. *Atg4b*-deficient mice showed impaired equilibrioception due to defects in the development of otoconia [33]. In contrast, *Map1lc3a*-deficient mice developed normally despite a total lack of LC3, and no obvious abnormalities were observed compared to wild-type mice, suggesting the existence of a new compensatory mechanism for the loss of LC3 [34]. The bone phenotype in *Atg4b*- or *Map1lc3a*-deficient mice has not been described, but the generation of osteoclast-specific *Atg4b*- or *Map1lc3a*-deficient mice may help clarify the physiological and pathological roles of the ATG4B/LC3 axis in osteoclastic bone resorption.

Our findings showed that the ATG4B inhibitor NSC185058 suppressed both RANKL-induced osteoclastogenesis and the bone-resorbing activity. Furthermore, local injection of NSC185058 suppressed bone loss by suppressing the osteoclast development induced by the ligature-induced periodontitis model. These findings, together with those from previous studies, suggest that ATG4B inhibitors may be a viable option for the treatment of periodontitis.

Authorship contributions

Fumitaka Hiura: Investigation, Formal analysis, Writing – original draft, Writing - review & editing. **Yuko Kawabata:** Supervision, Writing - review & editing. **Tsukasa Aoki:** Investigation, review & editing. **Akiko Mizokami:** Supervision, Writing - review & editing. **Eijiro Jimi:** Funding acquisition, Conceptualization, Writing - review & editing.

Funding

This study was supported by a research grant for the OBT Research Center from the Kyushu University (to E.J.) and from the Research Fellowship for Young Scientists (19J21202 to F.H.).

Declaration of competing interest

The authors have declared no conflicts of interest.

Acknowledgments

The authors thank Mr. Hiroshi Otowa for his technical assistance in data collection of histology, and Ms. Sakura Chishaki and Ms. Mayuko Inoue for maintaining mice. We would like to thank Japan Medical Communication (https://www.japan-mc.co.jp) for English language editing.

References

[1] N. Udagawa, M. Koide, M. Nakamura, Y. Nakamichi, T. Yamashita, S. Uehara, Y. Kobayashi, Y. Furuya, H. Yasuda, C. Fukuda, E. Tsuda E, Osteoclast differentiation by RANKL and OPG signaling pathways, J. Bone Miner. Metabol. 39 (1) (2021) 19–26, https://doi.org/10.1007/s00774-020-01162-6.
[2] M. Omi, Y. Mishina, Roles of osteoclasts in alveolar bone remodeling, Genesis 27 (2022), e23490, https://doi.org/10.1002/dvg.23490.
[3] Y. Yang, D.J. Klionsky, Autophagy and disease: unanswered questions, Cell Death Differ. 27 (3) (2020) 858–871, https://doi.org/10.1038/s41418-019-0480-9.
[4] C. He, Balancing nutrient and energy demand and supply via autophagy, Curr. Biol. 32 (2022) R684–R696, https://doi.org/10.1016/j.cub.2022.04.071.
[5] L. Zhang, J. Li, L. Ouyang, B. Liu, Y. Cheng, Unraveling the roles of Atg4 proteases from autophagy modulation to targeted cancer therapy, Cancer Lett. 373 (1) (2016) 19–26, https://doi.org/10.1016/j.canlet.2016.01.022.
[6] M. Li, Y. Hou, J. Wang, X. Chen, Z.M. Shao, X.M. Yin, Kinetics comparisons of mammalian Atg4 homologues indicate selective preferences toward diverse Atg8 substrates, J. Biol. Chem. 286 (9) (2011) 7327–7338, https://doi.org/10.1074/jbc.M110.199059.
[7] Z.Q. Yu, T. Ni, B. Hong, H.Y. Wang, F.J. Jiang, S. Zou, Y. Chen, X.L. Zheng, D.J. Klionsky, Y. Liang, Z. Xie, Dual roles of Atg8-PE deconjugation by Atg4 in autophagy, Autophagy 8 (6) (2012) 883–892, https://doi.org/10.4161/auto.19652.
[8] S. Cabrera, M. Maciel, I. Herrera, T. Nava, F. Vergara, M. Gaxiola, C. López-Otín, M. Selman, A. Pardo, Essential role for the ATG4B protease and autophagy in bleomycin-induced pulmonary fibrosis, Autophagy 11 (4) (2015) 670–684, https://doi.org/10.1080/15548627.2015.1034409.
[9] C.C. Proenca, N. Stoehr, M. Bernhard, S. Seger, C. Genoud, A. Roscic, P. Paganetti, S. Liu, L.O. Murphy, R. Kuhn, T. Bouwmeester, I. Galimberti, Atg4b-dependent autophagic flux alleviates Huntington's disease progression, PLoS One 8 (7) (2013), e68357, https://doi.org/10.1371/journal.pone.0068357.
[10] E. Tran, A. Chow, T. Goda, A. Wong, K. Blakely, M. Rocha, S. Taeb, V.C. Hoang, S.K. Liu, U. Emmenegger, Context-dependent role of ATG4B as target for autophagy inhibition in prostate cancer therapy, Biochem. Biophys. Res. Commun. 441 (4) (2013) 726–731, https://doi.org/10.1016/j.bbrc.2013.10.117.
[11] S. Wu, J. Su, H. Qian, T. Guo, SLC27A4 regulate ATG4B activity and control reactions to chemotherapeutics-induced autophagy in human lung cancer cells, Tumour Biol 37 (5) (2016) 6943–6952, https://doi.org/10.1007/s13277-015-4587-4.
[12] A. Montaseri, C. Giampietri, M. Rossi, A. Riccioli, A. Del Fattore, A. Filippini, The role of autophagy in osteoclast differentiation and bone resorption function, Biomolecules 10 (10) (2020) 1398, https://doi.org/10.3390/biom10101398.
[13] Y.F. Guo, T. Su, M. Yang, C.J. Li, Q. Guo, Y. Xiao, Y. Huang, Y. Liu, X.H. Luo, The role of autophagy in bone homeostasis, J. Cell. Physiol. 236 (6) (2021) 4152–4173, https://doi.org/10.1002/jcp.30111.
[14] F. Zach, F. Polzer, A. Mueller, A. Gessner, p62/sequestosome 1 deficiency accelerates osteoclastogenesis *in vitro* and leads to Paget's disease-like bone phenotypes in mice, J. Biol. Chem. 293 (24) (2018) 9530–9541, https://doi.org/10.1074/jbc.RA118.002449.
[15] C.J. DeSelm, B.C. Miller, W. Zou, W.L. Beatty, E. van Meel, Y. Takahata, J. Klumperman, S.A. Tooze, S.L. Teitelbaum, H.W. Virgin, Autophagy proteins regulate the secretory component of osteoclastic bone resorption, Dev. Cell 21 (5) (2011) 966–974, https://doi.org/10.1016/j.devcel.2011.08.016.
[16] Y.H. Chung, S.Y. Yoon, B. Choi, D.H. Sohn, K.H. Yoon, W.J. Kim, D.H. Kim, E.J. Chang, Microtubule-associated protein light chain 3 regulates Cdc42-dependent actin ring formation in osteoclast, Int. J. Biochem. Cell Biol. 44 (6) (2012) 989–997, https://doi.org/10.1016/j.biocel.2012.03.007.
[17] J.S. Becerra-Ruiz, C. Guerrero-Velázquez, F. Martínez-Esquivias, L.A. Martínez-Pérez, J.M. Guzmán-Flores, Innate and adaptive immunity of periodontal disease, from etiology to alveolar bone loss, Oral Dis. 28 (6) (2022) 1441–1447, https://doi.org/10.1111/odi.13884.
[18] Y. An, W. Liu, P. Xue, Y. Zhang, Q. Wang, Y. Jin, Increased autophagy is required to protect periodontal ligament stem cells from apoptosis in inflammatory microenvironment, J. Clin. Periodontol. 43 (7) (2016) 618–625, https://doi.org/10.1111/jcpe.12549.
[19] Y. Yang, Y. Huang, W. Li, Autophagy and its significance in periodontal disease, J. Periodontal. Res. 56 (1) (2021) 18–26, https://doi.org/10.1111/jre.12810.
[20] T. Abe, G. Hajishengallis, Optimization of the ligature-induced periodontitis model in mice, J. Immunol. Methods 394 (1–2) (2013) 49–54, https://doi.org/10.1016/j.jim.2013.05.002.
[21] N.Y. Lin, C.W. Chen, R. Kagwiria, R. Liang, C. Beyer, A. Distler, J. Luther, K. Engelke, G. Schett, J.H. Distler, Inactivation of autophagy ameliorates glucocorticoid-induced and ovariectomy-induced bone loss, Ann. Rheum. Dis. 75 (6) (2016) 1203–1210, https://doi.org/10.1136/annrheumdis-2015-207240.
[22] Y.H. Chung, Y. Jang, B. Choi, D.H. Song, E.J. Lee, S.M. Kim, Y. Song, S.W. Kang,

S.Y. Yoon, E.J. Chang, Beclin-1 is required for RANKL-induced osteoclast differentiation, J. Cell. Physiol. 229 (12) (2014) 1963–1971, https://doi.org/10.1002/jcp.24646.
[23] A. Arai, S. Kim, V. Goldshteyn, T. Kim, N.H. Park, C.Y. Wang, R.H. Kim, Beclin1 modulates bone homeostasis by regulating osteoclast and chondrocyte differentiation, J. Bone Miner. Res. 34 (9) (2019) 1753–1766, https://doi.org/10.1002/jbmr.3756.
[24] D. Akin, S.K. Wang, P. Habibzadegah-Tari, B. Law, D. Ostrov, M. Li, X.M. Yin, J.S. Kim, N. Horenstein, W.A. Dunn Jr., A novel ATG4B antagonist inhibits autophagy and has a negative impact on osteosarcoma tumors, Autophagy 10 (11) (2014) 2021–2035, https://doi.org/10.4161/auto.32229.
[25] J. Chu, Y. Fu, J. Xu, X. Zheng, Q. Gu, X. Luo, Q. Dai, S. Zhang, P. Liu, L. Hong, M. Li, ATG4B inhibitor FMK-9a induces autophagy independent on its enzyme inhibition, Arch. Biochem. Biophys. 644 (2018) 29–36, https://doi.org/10.1016/j.abb.2018.03.001.
[26] L. Zhong, B. Yang, Z. Zhang, J. Wang, X. Wang, Y. Guo, W. Huang, Q. Wang, G. Cai, F. Xia, S. Zhou, S. Ma, Y. Nie, J. Lei, M. Li, P. Liu, W. Deng, Y. Liu, F. Han, J. Wang, Targeting autophagy peptidase ATG4B with a novel natural product inhibitor Azalomycin F4a for advanced gastric cancer, Cell Death Dis. 13 (2) (2022) 161, https://doi.org/10.1038/s41419-022-04608-z.
[27] T. Tamura, N. Takahashi, T. Akatsu, T. Sasaki, N. Udagawa, S. Tanaka, T. Suda, New resorption assay with mouse osteoclast-like multinucleated cells formed in vitro, J. Bone Miner. Res. 8 (8) (1993) 953–960, https://doi.org/10.1002/jbmr.5650080808.
[28] E. Jimi, T. Shuto, T. Koga, Macrophage colony-stimulating factor and interleukin-1 α maintain the survival of osteoclast-like cells, Endocrinology 136 (2) (1995) 808–811, https://doi.org/10.1210/endo.136.2.7835314.
[29] Y.K. Kim, J.H. Ahn, M. Lee, Src family kinase inhibitor PP2 induces LC3 conversion in a manner that is uncoupled from autophagy and increases apoptosis in multidrug-resistant cells, Biomol. Ther. (Seoul). 20 (4) (2012) 393–398, https://doi.org/10.4062/biomolther.2012.20.4.393.
[30] I. Nakamura, N. Takahashi, T. Sasaki, S. Tanaka, N. Udagawa, H. Murakami, K. Kimura, Y. Kabuyama, T. Kurokawa, T. Suda, Y. Fukui, Wortmannin, a specific inhibitor of phosphatidylinositol-3 kinase, blocks osteoclastic bone resorption, FEBS Lett. 361 (1) (1995) 79–84, https://doi.org/10.1016/0014-5793(95)00153-z.
[31] I. Nakamura, T. Sasaki, S. Tanaka, N. Takahashi, E. Jimi, T. Kurokawa, Y. Kita, S. Ihara, T. Suda, Y. Fukui, Phosphatidylinositol-3 kinase is involved in ruffled border formation in osteoclasts, J. Cell. Physiol. 172 (2) (1997) 230–239, https://doi.org/10.1002/(SICI)1097-4652(199708)172:2<230::AID.
[32] S. He, Q. Zhou, B. Luo, B. Chen, L. Li, F. Yan, Chloroquine and 3-methyladenine attenuates periodontal inflammation and bone loss in experimental periodontitis, Inflammation 43 (1) (2020) 220–230, https://doi.org/10.1007/s10753-019-01111-0.
[33] G. Mariño, A.F. Fernández, S. Cabrera, Y.W. Lundberg, R. Cabanillas, F. Rodríguez, N. Salvador-Montoliu, J.A. Vega, A. Germanà, A. Fueyo, J.M. Freije, C. López-Otín, Autophagy is essential for mouse sense of balance, J. Clin. Invest. 120 (7) (2010) 2331–2344, https://doi.org/10.1172/JCI42601.
[34] G.M. Cann, C. Guignabert, L. Ying, N. Deshpande, J.M. Bekker, L. Wang, B. Zhou, M. Rabinovitch, Developmental expression of LC3α and β: absence of fibronectin or autophagy phenotype in LC3β knockout mice, Dev. Dynam. 237 (1) (2008) 187–195, https://doi.org/10.1002/dvdy.21392.